tion lengths, Schaefer et al. adopt the de Gennes reptation concept to obtain expressions for the variation of D_s with concentration. The weakness in this model lies in the identification of relationships between the correlation lengths. This particular aspect has recently been addressed by Muthukumar and Edwards,[26] who conclude that such identifications are not supported by theory for semidilute solutions of real (nonphantom) chains. Given these theoretical *caveats* the marginal solvent model does predict the appropriate asymptotic variation of dynamical parameters with concentration in the semidilute regime. Nonetheless the predicted discernable $D_s \sim c^{-2.5}$ behavior has not been observed here and would seem to have been too bold a distillation from the algebra. Both the marginal solvent and crossover modification to the de Gennes reptation theory predict M^{-2} scaling for D_s throughout the semidilute regime. However this relationship has been observed to prevail only in the high concentration asymptotic region labeled respectively Θ-like and Gaussian in the two models. Consequently the observed molar mass variation of D_s is not encompassed by any of the models proposed.

This inability of the models to predict the observed variation of self-diffusion with molar mass is a serious problem yet to be resolved. It would seem that the most likely reason for this is, as indicated by Muthukumar and Edwards, the lack of theoretical justification for assuming simple relationships between the various correlation lengths defined in semidilute solutions. Indeed Muthukumar and Edwards allow that a more complicated dependence may exist when they state that "the question of whether the entanglement constraints change the ratio of (dynamic to static) screening lengths only merely by a constant or by a functional dependence on concentration remains open".

Registry No. Polystyrene (homopolymer), 9003-53-6.

References and Notes

(1) Edwards, S. F.; Freed K. F. *J. Chem. Phys.* **1976**, *61*, 1189.
(2) Edwards, S. F. *J. Phys. A* **1975**, *8*, 1670.
(3) de Gennes, P.-G. *Macromolecules* **1976**, *9*, 587.
(4) de Gennes, P.-G. *Macromolecules* **1976**, *9*, 594.
(5) Brochard, F.; de Gennes, P.-G. *Macromolecules* **1977**, *10*, 1157.
(6) Schaefer, D. W.; Joanny, J. F.; Pincus, P. *Macromolecules* **1980**, *13*, 1280.
(7) Daoud, M.; Jannink, G. *J. Phys. (Paris)* **1976**, *37*, 973.
(8) Schaefer, D. W. *Polymer Prepr. Am. Chem. Soc., Div. Polym. Chem.* **1982**, *23*, 53.
(9) Farnoux, B.; Boué, F.; Cotton, J. P.; Daoud, M.; Jannink, G.; Nierlich, M.; de Gennes, P.-G. *J. Phys. (Paris)* **1978**, *39*, 77.
(10) Weill, G.; de Cloizeaux, J. *J. Phys. (Paris)* **1979**, *40*, 99.
(11) Pouyet, G.; Francois, J.; Dayantis, J.; Weill, G. *Macromolecules*, **1980**, *13*, 176.
(12) Callaghan, P. T.; Pinder, D. N. *Macromolecules*, **1981**, *14*, 1334.
(13) Callaghan, P. T.; Pinder, D. N. *Polym. Bull.* **1981**, *5*, 305.
(14) For $M > 2 \times 10^6$ PFGNMR can detect an admixed cooperative diffusion coefficient. Any influence from cooperative modes will be shown as a dependence of D_s on $(\Delta - (1/3)\delta)$.
(15) The manufacturers, Pressure Chemical Co., quote M_w = 390 000 daltons for this polymer. However it is apparent that D_0,[12] k_f,[12] and k_D[16] are more consistent with that expected by interpolation between neighboring molar masses if the true molar mass were 350 000 daltons.
(16) King, T. A.; Knox, A.; McAdam, J. D. G. *Polymer* **1973**, *14*, 293.
(17) Callaghan, P. T.; Trotter, C. M.; Jolley, K. W. *J. Magn. Reson.* **1980**, *37*, 247.
(18) Stejskal, E. O.; Tanner, J. E. *J. Chem. Phys.* **1965**, *42*, 288.
(19) Callaghan, P. T.; Le Gros, M.; Pinder, D. N. *J. Chem. Phys.* **1983**, *79*, 6372.
(20) Hervet, H.; Leger, L.; Rondelez, F. *Phys. Rev. Lett.* **1979**, *42*, 1681.
(21) Laurent, T. C.; Sundelöf, L. O.; Wik, K. V.; Wärmegåard, B. *Eur. J. Biochem.* **1976**, *68*, 95.
(22) Callaghan, P. T.; Pinder, D. N. *Macromolecules* **1983**, *16*, 968.
(23) Callaghan, P. T.; Pinder, D. N. *Macromolecules* **1980**, *13*, 1085.
(24) Amis, E. J.; Han, C. C. *Polymer* **1982**, *23*, 1403.
(25) Lêger, L.; Hervet, H.; Rondelez, F. *Macromolecules* **1981**, *14*, 1732.
(26) Muthumukar, M.; Edwards, S. F. *Polymer* **1982**, *23*, 345.

Computer Simulation of the Effect of Primitive Path Length Fluctuations in the Reptation Model

R. J. Needs

Cavendish Laboratory, University of Cambridge, Cambridge CB3 0HE, United Kingdom.

Received May 16, 1983

ABSTRACT: A dynamics of the primitive path of a reptating polymer is proposed. The dynamics are equivalent to a Metropolis algorithm. This dynamics allows fluctuations in the number of primitive path segments N about a mean of $\bar{N}$ obeying a distribution where the probability P of a primitive path of N segments is given by $P(N) \propto \exp(-3(N-\bar{N})^2/2\bar{N})$. The diffusion constant of the center of mass and the zero shear rate viscosity η_0 are calculated by computer simulation for $\bar{N}$ in the range 5–60. Although the viscosity is lowered by the inclusion of these fluctuations, the simulation data do not provide an explanation of the experimental $\eta_0 \propto \bar{N}^{3.4}$.

Introduction

The reptation model of de Gennes[1] has been successful in describing many of the viscoelastic properties of polymer melts. The most intriguing discrepancy is in the molecular weight dependence of the zero shear rate viscosity η_0. Experiments indicate[2] that η_0 is proportional to the molecular weight to a power about 3.4, while the reptation theory gives $\eta_0 \propto M^3$. Doi has argued[3] that these results can be reconciled by considering fluctuations in the length of the primitive path of the polymer, sometimes called breathing motions; see Figure 1.

In the reptation theory[1,4-8] the stress remaining at time t after a small strain at time 0 is proportional to the fraction $F(t)$ of original primitive path still occupied. This is related to the zero shear viscosity by

$$\eta_0 = G_N^\circ \int_0^\infty F(t)\, dt \tag{1}$$

where G_N° is the plateau modulus. Also the recoverable compliance J_e° is given by

$$J_e^\circ = G_N^\circ/\eta_0^2 \int_0^\infty tF(t)\, dt \tag{2}$$

0024-9297/84/2217-0437$01.50/0

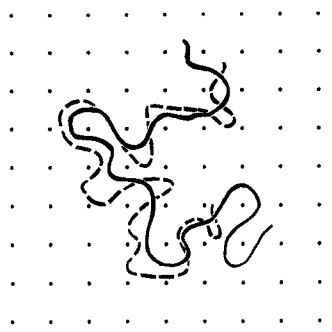

Figure 1. Dots represent fixed obstacles through which the polymer (continuous line) cannot pass. Some time later the polymer (dashed line) occupies a shorter length of primitive path.

Including fluctuations in the number of primitive path segments allows end segments of the original primitive path to be vacated more rapidly and thus lowers η_0. The effect might be expected to be important for a chain with a small mean number of primitive path segments $\bar{N}$ but unimportant for $\bar{N}$ large. Doi calculated[3,9] the probability distribution of a primitive path of N segments

$$P(N) \propto \exp(-3(N - \bar{N})^2/2\bar{N}) \tag{3}$$

He then calculated[3]

$$\eta_0 \propto \bar{N}^3((1 - \bar{N}^{-1/2})^3 + (1/5)\bar{N}^{-1.5}) \tag{4}$$

which closely resembles $\eta_0 \propto \bar{N}^{3.4}$ for $\bar{N}$ up to about 100, but his calculation is not exact and the effect seems worthy of further investigation.

In this paper a dynamics for the primitive path is used that obeys the distribution of eq 3. By computer simulation the viscosity and diffusion constant are calculated and compared with those for the constant primitive path length reptation model.

Primitive Path Dynamics

The primitive path of the polymer is a chain of N freely jointed rods or segments as in the Doi–Edwards model.[4] The essential difference of the fluctuating primitive path length dynamics used in this paper to the Doi–Edwards model is that the number of segments in the primitive path is a function of time. We use the idea of a Metropolis algorithm[10] to form the basis of a dynamics of the primitive path whose number of segments obeys the distribution of eq 3.

Suppose at some instant we have a path of N_1 segments. One of the following four choices is made at random: (1) add a segment to end 1; (2) add a segment to end 2; (3) subtract a segment from end 1; (4) subtract a segment from end 2. If the choice moves N_1 nearer to $\bar{N}$, we allow it. If the choice moves N_1 further from $\bar{N}$, we allow it with the probability Q, where

$$Q = \exp(3(N_1 - \bar{N})^2/2\bar{N} - 3(N_2 - \bar{N})^2/2\bar{N}) \tag{5}$$

and N_2 is the number of primitive path segments if the selected move were to take place. This weighting is accomplished by choosing a random number R between 0 and 1. If $R < Q$, we allow the move; otherwise we disallow it but count the attempted move as a time step. Obviously, the primitive path cannot have a negative length. If N_1 is zero and we choose to subtract a segment, then the move is disallowed and counted as a time step. Metropolis et al.[10] proved that such a procedure would ensure that the input distribution was preserved.

In the Doi–Edwards model[4-7] the time step for a single backward or forward shift of the primitive path is taken as proportional to the number of primitive path segments. To compare the dynamics used here with those of Doi and Edwards, we need to define the $\bar{N}$ dependence of the time step for our fluctuating path dynamics. Initially, we shall assume that this time step is proportional to $\bar{N}$.

If the number of segments in the chain is N, then $P(N,t)$, the probability of having N segments at time t, obeys a diffusion equation in a harmonic potential with a diffusion constant $D_{\bar{N}} \sim 1/\bar{N}$ and potential $3(N - \bar{N})^2/2\bar{N}$. The presence of the potential does not affect the $\bar{N}$ dependence of the time for a fluctuation τ, which is the time for a chain initially of $\bar{N}$ segments to have a significant probability of having $\bar{N} \pm \bar{N}^{1/2}$ segments, where the standard deviation of the distribution $\sim \bar{N}^{1/2}$. Thus we have that $\tau \sim (\bar{N} \pm \bar{N}^{1/2} - \bar{N})^2/D_{\bar{N}} \sim \bar{N}^2$. Thus the time for a fluctuation τ, or longest breathing mode, scales like the Rouse time, i.e., $\sim\bar{N}^2$. This is an essential feature of any reasonable dynamics.

In the dynamics of the primitive path of a real polymer, if a move took a segment off end 1, then the next move is more likely to add a segment to end 1 than end 2, as the time between moves $\sim \bar{N}$ while the equilibrium time for the fluctuations in monomer density along the primitive path $\sim \bar{N}^2$. Similarly, if we add a segment to end 1, the next move is more likely to subtract a segment from end 1 than end 2. This memory effect is not included in these dynamics. These two types of move are given less weight in the dynamics proposed than is correct, but neither of them can reduce the stress, so it seems unlikely that the viscosity will be reduced by the inclusion of this memory effect.

Simulation of Viscosity

The stress tensor $\sigma_{\alpha\beta}$ used by Doi and Edwards[5,11] is given by

$$\sigma_{\alpha\beta} \propto \left\langle \sum_i \frac{r_{i\alpha}r_{i\beta}}{m_i b^2} \right\rangle \tag{6}$$

where $r_{i\alpha}$ is the αth component of the end-to-end vector of the ith primitive path segment, m_i is the number of Rouse segments of the real chain in the ith primitive path segment, and b is the Rouse step length of the real chain. If $N(t)$ is the number of primitive path segments at time t, then $m_i \propto \bar{N}/N(t)$. The primitive path segments that have left the original tube do not contribute to the stress, and thus the stress from a single chain is

$$\sigma(t) \propto n(t)N(t)/\bar{N} \tag{7}$$

where $n(t)$ is the number of primitive path segments at time t that are still in the original tube. The average number of chains per unit volume is $1/\bar{N}$; thus

$$\eta_0 \propto \int_0^\infty n(t)N(t)\, dt/\bar{N}^2 \tag{8}$$

Here we note that if we use the average value of m_i, i.e., put $N(t) = \bar{N}$, we find no significant difference in the simulation results for $\bar{N} > 10$ but for small $\bar{N}$, η_0 is slightly raised, the maximum effect being for the smallest $\bar{N}$ of 5 when η_0 is raised by about 4.5%.

The model used here is discrete in both space and time; by that, we mean that the number of primitive path segments takes only integral values and attempted moves of the chain take place at instants separated in time by a constant time step. Rewriting eq 8 as a sum over time steps, we have, as the time step is proportional to $\bar{N}$

$$\eta_{0f} \propto \sum_j n_j N_j/\bar{N} \tag{9}$$

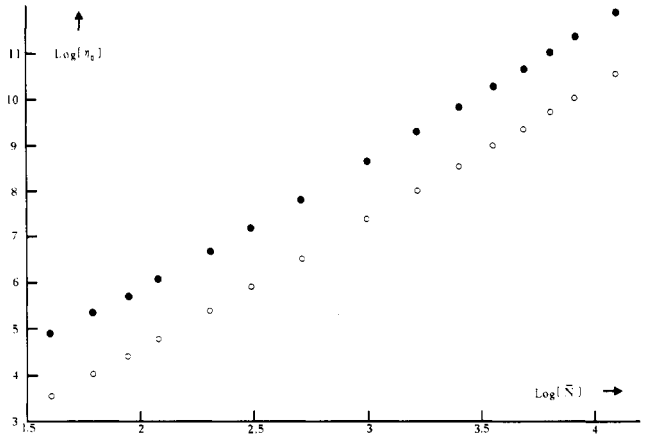

Figure 2. ln (viscosity) against ln (mean primitive path length).

Table I
Viscosity and Recoverable Compliance of the Fluctuating Path Length Dynamics

$\bar{N}$	η_{0f}	$J_e^\circ G_N^\circ \eta_{0f}^2$
5	(1.36 ± 0.02) × 10^2	(1.96 ± 0.06) × 10^4
6	(2.12 ± 0.05) × 10^2	(4.77 ± 0.20) × 10^4
7	(3.09 ± 0.04) × 10^2	(1.05 ± 0.03) × 10^5
8	(4.41 ± 0.09) × 10^2	(2.19 ± 0.11) × 10^5
10	(8.04 ± 0.10) × 10^2	(7.37 ± 0.17) × 10^5
12	(1.33 ± 0.02) × 10^3	(2.10 ± 0.05) × 10^6
15	(2.45 ± 0.03) × 10^3	(7.31 ± 0.22) × 10^6
20	(5.61 ± 0.09) × 10^3	(3.85 ± 0.15) × 10^7
25	(1.07 ± 0.01) × 10^4	(1.40 ± 0.05) × 10^8
30	(1.82 ± 0.02) × 10^4	(4.03 ± 0.12) × 10^8
35	(2.82 ± 0.03) × 10^4	(9.74 ± 0.22) × 10^8
40	(4.17 ± 0.06) × 10^4	(2.14 ± 0.05) × 10^9
45	(5.99 ± 0.08) × 10^4	(4.41 ± 0.13) × 10^9
50	(8.22 ± 0.01) × 10^4	(8.37 ± 0.24) × 10^9
60	(1.40 ± 0.02) × 10^5	(2.39 ± 0.09) × 10^{10}

The subscript f denotes fluctuating path length dynamics. Also from eq 1 and 2 the recoverable compliance J_e° is given by

$$J_e^\circ \propto \sum_j j n_j N_j / \eta_0^2 \tag{10}$$

and the dimensionless product $J_e^\circ G_N^\circ$ is

$$J_e^\circ G_N^\circ = \frac{\sum_j j n_j N_j}{(\sum_j n_j N_j / \bar{N})^2} \tag{11}$$

To calculate the viscosity by computer simulation, we first of all pick an initial number of primitive path segments from the distribution of eq 3. Then we attempt moves via the Metropolis algorithm already described. After each move we recalculate n_j and N_j until $n_j = 0$; i.e., the chain has completely left its original tube. Using n_j and N_j, we calculate the sums in eq 9 and 10. For each value of $\bar{N}$, 10 runs were carried out, each averaging over 1000 chains. The viscosity results are plotted in Figure 2; they are also tabulated in Table I together with the recoverable compliance data, because the full accuracy of the data cannot be reconstructed from Figure 2.

It is important to realize that a discrete space and time version of the Doi–Edwards model does not give $\eta_0 \propto \bar{N}^3$ for small $\bar{N}$, where $\bar{N}$ is not now a fluctuating quantity. The results of Doi and Edwards[4-7] are solutions of differential equations; they treated time and the arc coordinate of the primitive path as continuous variables. Here we seek solutions of the corresponding discrete equations

Table II
Viscosity and Recoverable Compliance of the Nonfluctuating Path Length Dynamics

$\bar{N}$	η_0	$J_e^\circ G_N^\circ \eta_0^2$
5	(3.49 ± 0.06) × 10^1	(1.11 ± 0.04) × 10^3
6	(5.64 ± 0.07) × 10^1	(3.08 ± 0.10) × 10^3
7	(8.40 ± 0.15) × 10^1	(7.04 ± 0.29) × 10^3
8	(1.19 ± 0.01) × 10^2	(1.44 ± 0.04) × 10^4
10	(2.20 ± 0.03) × 10^2	(5.09 ± 0.13) × 10^4
12	(3.66 ± 0.06) × 10^2	(1.45 ± 0.06) × 10^5
15	(6.80 ± 0.06) × 10^2	(5.16 ± 0.09) × 10^5
20	(1.54 ± 0.02) × 10^3	(2.67 ± 0.06) × 10^6
25	(2.94 ± 0.04) × 10^3	(9.92 ± 0.27) × 10^6
30	(4.98 ± 0.10) × 10^3	(2.87 ± 0.15) × 10^7
35	(7.81 ± 0.13) × 10^3	(7.11 ± 0.29) × 10^7
40	(1.15 ± 0.01) × 10^4	(1.53 ± 0.05) × 10^8
45	(1.63 ± 0.02) × 10^4	(3.14 ± 0.12) × 10^8
50	(2.22 ± 0.04) × 10^4	(5.75 ± 0.13) × 10^8
60	(3.78 ± 0.07) × 10^4	(1.69 ± 0.07) × 10^9

with which to compare our fluctuating path length results. In this paper the viscosity of the discrete version of the Doi–Edwards dynamics is computer simulated. We use eq 12 to calculate the viscosity, the difference from eq 9 being that now $N_j = \bar{N}$

$$\eta_0 \propto \sum_j n_j \tag{12}$$

Also

$$J_e^\circ \propto \sum_j j n_j \bar{N} / \eta_0^2 \tag{13}$$

The other details of the simulation are the same as for the fluctuating dynamics and the results are plotted in Figure 2 and tabulated in Table II.

Simulation of the Diffusion Constant of the Center of Mass

The simulation of the diffusion constant of the center of mass was performed on a cubic lattice. This enables a more efficient computer program to be written. The problem of the calculation of the viscosity reduces to one dimension, the arc coordinate of the primitive path. The reason for this is that to calculate the stress at time t we need only know the number of segments in the original primitive path, i.e., at time 0, and the total number of segments at time t, not their coordinates. To calculate the diffusion constant we define the center of mass coordinate r_{cm} of the chain as

$$r_{cm} = \frac{1}{N+1} \sum_i r_i \tag{14}$$

where the r_i are the $N + 1$ coordinates of the end points of the N segments. To calculate the diffusion constant we measure the displacement squared of the center of mass from its original position as a function of time. This was averaged over 500 chains and a least-squares fit gave the diffusion constant D_f. Ten such runs were done for each value of $\bar{N}$. In each run the displacement squared of the center of mass was greater than 30 segment lengths squared. The results are plotted in Figure 3.

The diffusion constant D of the discrete form of the Doi–Edwards model can be calculated by using the method of ref 4. We find

$$D = \frac{1}{(\bar{N}+1)\bar{N}} \tag{15}$$

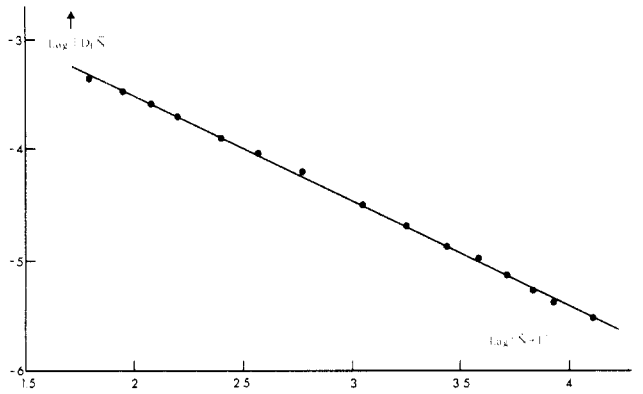

Figure 3. ln $(D_f\bar{N})$ against ln $(\bar{N} + 1)$. Regression line of eq 16 indicated.

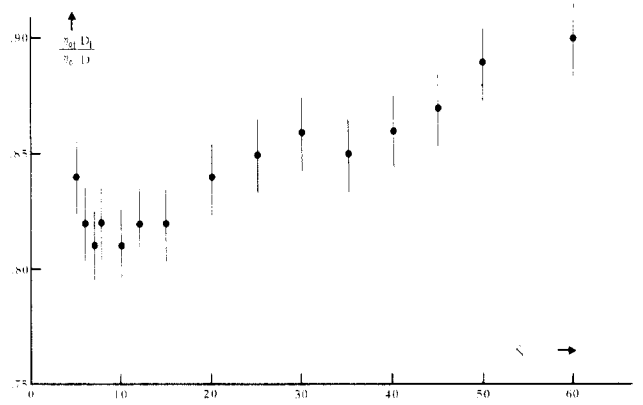

Figure 4. Ratio of the viscosities with the time step altered so that the diffusion constants of the two models are equal against $\bar{N}$. Error bars of 1 standard deviation are indicated.

The function $D_f(\bar{N})$ was fitted by a least-squares method to the form

$$D_f = \frac{A}{(\bar{N} + 1)^B \bar{N}} \tag{16}$$

The single power of $\bar{N}$ was introduced by the time step and we preserve this in the fit. We obtain

$$A = 0.198 \pm 0.006$$
$$B = 0.95 \pm 0.01 \tag{17}$$

Conclusions and Discussion

A possible way of analyzing the simulation data is to define the time step for the fluctuating dynamics so that the diffusion constants for the fluctuating and nonfluctuating dynamics are equal. If we do this, we find that the viscosity from the fluctuating dynamics is lower than that for the nonfluctuating dynamics by between 10 and 20%. In Figure 4 the equal diffusion constant viscosity ratio $(\eta_{0f}D_f)/(\eta_0 D)$ is plotted against $\bar{N}$, where D and D_f are taken from eq 15 and 16, respectively. As $\bar{N}$ increases from 10 to 60, $\eta_{0f}D_f/\eta_0 D$ increases from about 0.8 to 0.9. Thus we have an increase in the viscosity exponent due to the fluctuations in path length of log (0.9/0.8)/log (60/10) = 0.066. We conclude that the primitive path dynamics postulated in this paper, which allow fluctuations in the length of the primitive path, do not provide an explanation of the experimental law $\eta_0 \propto M^{3.4}$.

It is important to note that we cannot conclude that these results are in disagreement with the form of Doi's result for the viscosity in eq 4 in the limit of large $\bar{N}$. In Figure 5 we plot $\{(\eta_{0f}D_f)/(\eta_0 D)\}^{1/3}$ against $\bar{N}^{-1/2}$. According to eq 4, if we neglect the term $(1/5)\bar{N}^{-1.5}$, which is very small, we should get a straight line of gradient −1. Remembering that at $\bar{N}^{-1/2} = 0$, we should get $\{(\eta_{0f}D_f)/(\eta_0 D)\}^{1/3} = 1$; we see that for large $\bar{N}$ the simulation data are fitted well by

$$(\eta_{0f}D_f/\eta_0 D) \cong (1 - 0.29\bar{N}^{-1/2})^3 \tag{18}$$

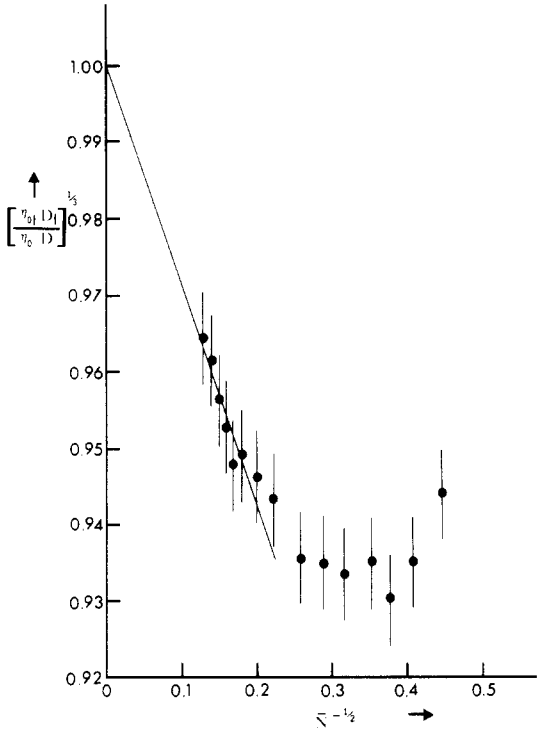

Figure 5. $(\eta_{0f}D_f/\eta_0 D)^{1/3}$ against $\bar{N}^{-1/2}$. A slope of −0.29 through the point (0, 1) is shown. Error bars of 1 standard deviation are indicated.

Table III
Product of the Recoverable Compliance J_e° and Plateau Modulus G_N° as a Function of $\bar{N}$

$\bar{N}$	$J_e^\circ G_N^\circ$ fluctuating dynamics	$J_e^\circ G_N^\circ$ nonfluctuating dynamics
5	1.06	0.91
6	1.07	0.97
7	1.10	1.00
8	1.13	1.02
10	1.14	1.05
12	1.19	1.09
15	1.22	1.12
20	1.22	1.13
25	1.22	1.15
30	1.22	1.15
35	1.23	1.17
40	1.23	1.16
45	1.23	1.17
50	1.23	1.17
60	1.22	1.19

The values of $J_e^\circ G_N^\circ$ are tabulated in Table III for both the fluctuating and nonfluctuating primitive path length dynamics. For the nonfluctuating dynamics the value rises from 0.91 for small $\bar{N}$ and approaches the Doi–Edwards value of 1.2 for large N. For the fluctuating dynamics $J_e^\circ G_N^\circ$ rises from 1.06 for small $\bar{N}$ to a constant value of just over 1.2 for large $\bar{N}$.

Acknowledgment. The author thanks Professor W. W. Graessley for the suggestion in ref 8 that a computer simulation of this problem would be useful and Dr. R. C. Ball and Professor S. F. Edwards for useful discussions. The author acknowledges the assistance of an SERC CASE

award with ICI, Welwyn Garden City, U.K.

References and Notes

(1) P.-G. de Gennes, *J. Chem. Phys.*, **55**, 572 (1971).
(2) J. D. Ferry, "Viscoelastic Properties of Polymers", 3rd ed., Wiley, New York, 1980, p 244.
(3) M. Doi, *J. Polym. Sci., Polym. Lett. Ed.*, **19**, 265 (1981).
(4) M. Doi and S. F. Edwards, *J. Chem. Soc., Faraday Trans. 2*, **74**, 1798 (1978).
(5) M. Doi and S. F. Edwards, *J. Chem. Soc., Faraday Trans. 2*, **74**, 1802 (1978).
(6) M. Doi and S. F. Edwards, *J. Chem. Soc., Faraday Trans. 2*, **74**, 1818 (1978).
(7) M. Doi and S. F. Edwards, *J. Chem. Soc., Faraday Trans. 2*, **75**, 38 (1979).
(8) W. W. Graessley, *Adv. Polym. Sci.*, **47** (1982).
(9) M. Doi and N. Y. Kuzuu, *J. Polym. Sci., Polym. Lett. Ed.*, **18**, 775 (1980).
(10) N. Metropolis, A. Rosenbluth, M. Rosenbluth, A. Teller, and E. Teller, *J. Chem. Phys.*, **21**, 6 (1953).
(11) R. B. Bird, R. C. Armstrong, O. Hassager, and C. F. Curtiss, "Dynamics of Polymeric Liquids", Wiley, New York, 1977, Vol. 1 and 2.

Effect of Cross-Bridge Motion on the Spectrum of Light Quasielastically Scattered from *Limulus* Thick Myofilament Suspensions

Satoru Fujime*† and Kenji Kubota‡

Mitsubishi-Kasei Institute of Life Sciences, Machida, Tokyo 194, Japan, and Department of Physics, Ochanomizu University, Bunkyo, Tokyo 112, Japan. *Received June 8, 1983*

ABSTRACT: A thick myofilament has many projections called cross-bridges. In order to see the effect of cross-bridge motion on the spectrum of light quasielastically scattered from suspensions of isolated thick myofilaments, a theoretical model for a semiflexible filament[2] is extended to a situation where each projection from the filament undergoes thermal fluctuations around its mean position. If activation by calcium ions would result in an increase of the flexibility of some part(s) of each projection, our simple model could account for the most part for the excess line width in the activated state over that in the relaxed/rerelaxed one observed for *Limulus* thick myofilament suspensions.[1] On the basis of the same experimental result, we estimated the flexibility parameter of the *Limulus* thick myofilament in the relaxed/rerelaxed state.

Introduction

The main aim of this paper is to discuss a possible contribution of motions of projections (cross-bridges) to the line widths of the spectra observed by Kubota et al.[1] for *Limulus* thick myofilament suspensions. Figure 1 sketches one of their results. From this figure, we know that at $K^2 = 10 \times 10^{10}$ cm^{-2}

$$\bar{\Gamma}/K^2 \simeq 6D_1 \quad \text{(in a relaxed state)}$$
$$\bar{\Gamma}/K^2 \simeq 10D_1 \quad \text{(in an activated state)}$$
$$\bar{\Gamma}/K^2 \simeq 4D_1 \quad \text{(in a rerelaxed state)} \qquad (1)$$

where $\bar{\Gamma}$ is the average line width, K is the length of the momentum transfer vector, D and D_1 are respectively the overall and the sideways translational diffusion constants of a single thick filament and $D_1 = (3/4)D$ in the long-rod limit.

In another paper,[2] we showed that the limiting form of the first cumulant, $\bar{\Gamma}$, of the correlation function $G^1(\tau)$ for a very long and semiflexible filament is given by

$$\bar{\Gamma}/K^2 \to [D - (1/3)(D_3 - D_1)] + (L^2/12)\Theta + \frac{k_BT}{\zeta L}\sum_m{}''1 \quad \text{(when } KL \gg 1) \qquad (2)$$

where $D = (2D_1 + D_3)/3$, D_3 is the lengthways translational diffusion constant of the filament, L is its length, and $\sum''1$ means the number of bending modes of motion involved in the scattering process. When we take the long-rod limit of diffusion constants, i.e., $D_3 = 2D_1$, $D - {}^1/_3(D_3 - D_1) = D_1$, $(L^2/12)\Theta = D_1$, and $k_BT/\zeta L = D_1$, eq 2 is written as

$$\bar{\Gamma}/K^2 \to D_1 + D_1 + D_1\sum_m{}''1 \quad \text{(when } KL \gg 1) \qquad (3)$$

Equation 3 tells us that each mode of motion contributes to $\bar{\Gamma}/K^2$ by D_1 in the limit of $KL \gg 1$. For a very long filament with a slight flexibility we can expect that $\sum''1 = 2$–3 at the highest accessible K value. Actually, the length of a *Limulus* thick filament is 4 μm in the relaxed state and 3 μm in the activated/rerelaxed state. Thus, we may have $\bar{\Gamma}/K^2 = (4$–$5)D_1$ at, say, $K^2 = 10 \times 10^{10}$ cm^{-2}. This estimation can explain the experimental results of thick myofilaments in the relaxed/rerelaxed state (for details, see Appendix A). On the other hand, if we try to explain $\bar{\Gamma}/K^2 = 10D_1$ on the basis of eq 3, we have to assume a nonrealistic value for the filament flexibility. Thus, we have to seek another mode of motion which gives an extra line width of about $6D_1$.

Calcium ions induce the extra line width[1]. In addition to this, the following facts have already been shown.[3,4] Congo Red, which can shorten isolated myofibrils in the relaxing solution, also increases the $\bar{\Gamma}$ value. After heat denaturation or cleavage of the S1 moiety with papain, calcium ions do not increase the $\bar{\Gamma}$ value. The dramatic increase in $\bar{\Gamma}$ is also suppressed by treating the filaments with a myosin ATPase inhibitor such as vanadate ions or by replacing ATP with Cr-ADP. These results clearly indicate that the extra line width comes mostly from an "activated" motion of cross-bridges.

In what follows, we consider a simple model where the core of the thick filament is assumed to be a rigid rod and each projection from the core fluctuates around its mean position. The former assumption does not impose any serious restriction on the present problem, because the limiting value of $\bar{\Gamma}/K^2$ is a simple sum of various contri-

† Mitsubishi-Kasei Institute of Life Sciences.
‡ Ochanomizu University.

0024-9297/84/2217-0441$01.50/0